Microwave absorption by nanostructural ferric oxide encapsulated within MCM-41

Haiquan Guo,[a] **Wei Xu,**[a] **Min-Hui Cui,**[b] **Nan-Loh Yang**[b] **and Daniel L. Akins**[*a]

[a] *Center for Analysis of Structures and Interfaces (CASI), Chemistry Department, The City College of New York, Convent Ave. at 138th St., New York, NY 10031, USA. E-mail: akins@sci.ccny.cuny.edu; Fax: +1 212 650 6848; Tel: +1 212 650 6953*

[b] *Chemistry Department, The College of Staten Island, 2800 Victory Blvd., Staten Island, NY 10314, USA. E-mail: yang-n@postbox.csi.cuny.edu; Fax: +1 718 982 3910; Tel: +1 718 982 3899*

A new functional material with nonzero microwave absorption ability at zero applied magnetic field results from loading MCM-41 to a high percentage by weight with ferric oxide.

Ferric oxide (Fe_2O_3) is a technologically important substance with wide utility in the semiconductor, pigment, magnetic storage, nonlinear optics, catalyst and gas-sensor arenas.[1] Enhanced interest, of late, has centered on nanostructural Fe_2O_3, whose electronic and optoelectronic properties—as a result of both quantum confinement and the greater influence of surface states—may differ substantially from those of the bulk material.[2]

Synthetic approaches for forming nanostructural Fe_2O_3 have been varied. And with the discovery of the M-41S mesoporous materials family, research efforts have aimed to encapsulate Fe_2O_3 within, in particular, MCM-41, in order to develop "green" catalyst and semiconductor nanoparticles.[2–4] In the present paper, we report the development of a new functional nanocomposite material (MCM-41 loaded at a high level with Fe_2O_3), whose functionality involves an enhanced absorption of microwave energy, even in the absence of an applied magnetic field.

We prepared nanocomposite samples with different amounts of Fe_2O_3 loaded into the channels. The overall method involved, typically, synthesizing MCM-41 (by a method reported in the literature),[5]† but not calcining it, thus allowing the organic template to remain in the mesoporous channels. The external surface was then passivated with phenyltrimethoxysilane (*i.e.*, $C_6H_5Si(OCH_3)_3$).[6] The organic template within the pores was then extracted with ethanol and the internal surface of the MCM-41 functionalized using 3-(2-aminoethylamino)propyl-tri-methoxysilane (*i.e.*, $(CH_3O)_3Si(CH_2)_3NH(CH_2)_2NH_2$).[7–8] Ferric ions from a ferric nitrate ethanolic solution (0.1 M) were next incorporated into the channels of the above modified MCM-41 using two methods to control the levels of loading of the guest within the host MCM-41. For the low-load sample, the "incipient wetness" method was used, in which Fe^{3+} ions simply exchanged with the functionalizing agent. The sample was then centrifuged, and the supernatant solution was decanted. The precipitate was washed and then heated at 180 °C for 24 h. In the case of the high-load sample, the mixture of MCM-41 and ethanolic ferric nitrate was vigorously stirred and evaporated to remove ethanol. The sample was then washed and heated at 180 °C for *ca.* 24 h. The net effect is to enhance the amount of Fe_2O_3 formed within the channels of MCM-41.‡

X-ray diffraction spectra were acquired to examine the effect of encapsulation of Fe_2O_3 on the ordered structure of MCM-41. For the uncalcined as well as the functionalized MCM-41, three peaks are found (see Figure 1; spectra A and B) that can be indexed to (100), (110) and (200). For uncalcined MCM-41, the d_{100} spacing is calculated (using the Bragg equation) to be *ca.* 33 Å. After functionalization, the structure of the mesoporous material is found to be maintained, and the pore size is determined by N_2 adsorption/desorption to be *ca.* 24 Å.

Upon loading with Fe_2O_3, the XRD spectra of the composite exhibit changes. When the loading is high, the intensity of (100)
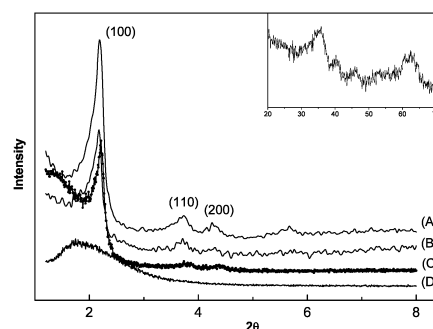

Fig. 1 XRD of (A) uncalcined MCM-41, (B) uncalcined and functionalized MCM-41, (C) low-load composite Fe_2O_3/MCM-41, and (D) high-load composite Fe_2O_3/MCM-41. Inset shows the large angle XRD of the high load sample.

peak is significantly decreased and broadened compared to that of low-load sample (see Figure 1, spectrum D). This suggests that with increased loading the structure of MCM-41 is distorted. From the large angle XRD pattern of the high-load composite (see inset in Figure 1), the guest inside MCM-41 is identified as being α-Fe_2O_3. The low-load composite does not support a large angle XRD spectrum, consonant with the idea that the nanoparticles formed are of extremely small diameters.[4]

By comparing the IR spectrum of MCM-41 samples (see Figure 2) before (A) and after encapsulation of Fe_2O_3 (B) and (C), we find that the spectra become simpler after encapsulation. IR bands at 1630, 1378, 790, 560, and 460 cm^{-1}, are essentially unchanged upon occlusion of Fe_2O_3. These bands are likely associated with the external passivating agent and surface vibrations of the mesoporous lattice. Some bands are observed to shift, such as 1074 cm^{-1} to 1090 cm^{-1}, attributed to the Si–O–Si vibration, and 976 cm^{-1} to 959 cm^{-1}, attributed to the Si–OH group; some bands exhibit lowered intensity upon formation of the composite, *i.e.*, the 2854 and 2918 cm^{-1} bands; while still other bands, in the case of the high-load sample, disappear: the bands at 1569, 1484, 1316, 1225, 698, and 666 cm^{-1} in spectrum A of Figure 2 vanish. These latter bands are
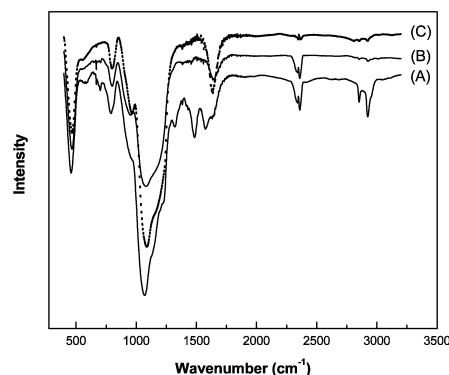

Fig. 2 IR spectrum of (a) functionalized MCM-41; (b) low-load MCM-41/Fe_2O_3; (c) high-load MCM-41/Fe_2O_3.

attributable by us to the stretching vibrations of C–H, Si–C, C–N, and the bending vibration for –NH$_2$. In the case of the low-load sample, some of the aforementioned bands, such as 1569, 1484 and 666 cm^{-1} remain, although with lowered intensities.

The above IR measurements are interpreted as indicating that with the treatments discussed, Fe$_2$O$_3$ is incorporated inside the mesoporous channels of MCM-41, resulting in constricted motion associated with the limit space. However, when the loading is low, the size of particles is sufficiently small that the vibrations are largely unimpeded.

Diffuse reflectance (DR) UV-Vis spectra of the low-load and high-load samples, as well as that of a ferric nitrate solution are shown in Figure 3. Both composite samples exhibit blue shifts in their band edges, when compared to the bulk Fe$_2$O$_3$, which has a band edge at *ca*. 560 nm.[4] For the low-load sample, the absorption spectrum mimics that of the ferric nitrate solution, and has a band edge near 350 nm. The high-load sample, on the other hand, exhibits a strong absorption peak at 392 nm. The large blue shifts in band edge position as referenced to the band edge of bulk Fe$_2$O$_3$ are associated with formation of nano-dimensioned entities within the mesoporous material. We further note that the high-load composite possesses a band at *ca*. 530 nm (shoulder) that likely indicates the presence of elongated structures.

Lastly, we describe the first-derivative EPR spectra for the composite system (see Figure 4). A broad EPR first-derivative signals of *g* value ~ 2.1 is observed for both samples. The low-load sample also exhibits a distinct signal at *g* ~ 4.3, corresponding to Fe^{3+} that is located at either strongly distorted rhombic sites located on the surface or isolated and dispersed in the pores.[9] We observed, further, that the high-load sample shows significant absorption at a magnetic field of ~ 99 G, and even extrapolates to non-zero absorption at zero applied field; this non-zero absorption phenomenon is not observed for the low-load sample. Moreover, the microwave absorption by the high-load sample was indicated by the decrease of the *Q* factor by 50% (at 99 G) compared with the control, and this decrease

in *Q* was substantially less for the low-load composite. Thus, Fe$_2$O$_3$ encapsulated in MCM-41 was demonstrated to show strong microwave absorption ability in the absence of an external magnetic field. We suspect some degree of alignment of the magnetic dipole moments within the nanosized, one-dimensional pores in the high-load sample, the result of the directed growth, under nano-dimensioned confinement, even in the absence of an external magnetic field. The origin of the zero-field absorption can be attributed to the high local field due to this alignment; a conclusion consistent with our observation of an increase in the *g* value of the absorption (near *g* ~ 2.1) with decrease in temperature, *i.e.*, an increase in the local field due to a higher order of alignment at a lower level of thermal randomization.

We have also undertaken preliminary investigation of the microwave spectrum that gives rise to the measured absorption. These latter studies have indicated that the peak absorption occurs in the 30 GHz region.

Further exploration of the structure/properties relationship in these materials may result in fundamental understanding of nanomagnets with high aspect ratio in spatially confined one-dimensional systems, and contribute to the technology of microwave shielding, including stealth technology. Apparently, the high aspect ratio is an important factor, since Fe$_2$O$_3$ nanoparticles with low aspect ratios do not show zero-field microwave absorption.[10]

In summary, Fe$_2$O$_3$ was encapsulated by two methods inside MCM-41, which has a one-dimensional, uniform pore structure of nano-dimensioned scale. Composite samples were characterized by UV-Vis, IR, EPR and X-ray diffraction. We have found, in general, that the pore size of MCM-41 and the loading level of Fe$_2$O$_3$ significantly affect the spectral properties of encapsulated ferric oxide. EPR indicates that for sufficient loading with Fe$_2$O$_3$, the composite material exhibits non-zero absorption at zero applied magnetic field and a substantial microwave absorption capability.

Notes and references

Fig. 3 (A) UV-Vis spectra of Fe(NO$_3$)$_3$ in ethanol solvent; (B) DR UV-Vis of low-load composite of Fe$_2$O$_3$ occluded within MCM-41; and (C) same as (B) except for high-load composite.
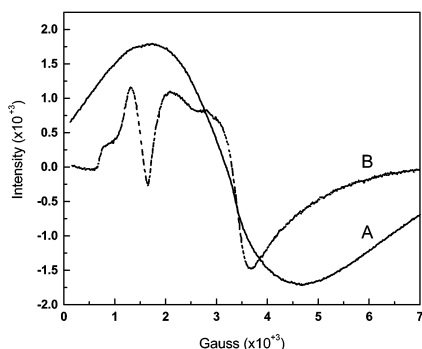
Fig. 4 Single scan first-derivative EPR spectra from 99.15 G to 7099.15 G of: (A) high-load composite of Fe$_2$O$_3$ occluded within MCM-41, and (B) low-load composite sample same composite.

1 L. Huo, W. Li, L. Lu, H. Cui, S. Xi, J. Wang, B. Zhao, Y. Shen and Z. Lu, *Chem. Mater.*, 2000, **12**, 790.
2 M. M. Iwamoto, T. Abe and Y. Tachibana, *J. Mol .Catal. A: Chem.*, 2000, **155**, 143.
3 T. Abe, Y. Tachibana, T. Uemastu and M. Iwamoto, *J. Chem. Soc., Chem. Commun.*, 1995, 1617.
4 L. Zhang, G. C. Papaefthymiou and J. Y. Ying, *J. Phys. Chem. B.*, 2001, **105**, 7414.
5 A. Sayari, C. Danumah and I. L. Moudrakovski, *Chem. Mater.*, 1995, **7**, 813; A. Sayari, I. L. Moudrakovski, C. Danumah, C. I. Ratcliffe, J. A. Ripmeester and K. F. Preston, *J. Phys. Chem.*, 1995, **99**, 16373.
6 Z. Zhang, S. Dai, X. Fan, D. A. Blom, S. J. Pennycook and Y. Wei, *J. Phys. Chem. B.*, 2001, **105**, 6755.
7 A. B. Bourlinos, A. Simopoulos, N. Boukos and D. Petridis, *J. Phys. Chem. B.*, 2001, **105**, 7432.
8 J. F. Diaz, K. J. Balkus Jr., F. Bedioui, V. Kurshev and L. Kevan, *Chem. Mater.*, 1997, **9**, 61.
9 L. Zhang, G. C. Papaefthymiou and J. Y. Ying, *J. Phys. Chem. B.*, 1998, **102**, 7721.
10 K. V. P. M. Shafi, A. Ulman, A. Dyal, X. Yan, N.-L. Yang, C. Estournès, L. Fournès, A. Wattiaux, H. White and M. Rafa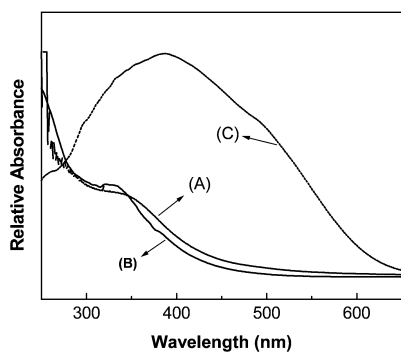ilovich, *Chem. Mater.*, 2002, **14**, 1778.